$Na_2(C_4O_4)(H_3BO_3)(H_2O)_4 \cdot H_3BO_3$: The First Borate–squarate with Strong SHG Response Reduced from Superior Synergy

Dong Yan,*[ab] Yao Ma,[a] Hongbo Huang,[e] Bingbing Zhang,*[e] Ru-Ling Tang,[d] Liang Hu,[a] Fei-Fei Mao,[bc] Jie Zheng,[a] Xiu-Du Zhang,[a] and Shu-Fang Li *[ab]

[a]*Key Laboratory of Functional Molecular Solids, Ministry of Education, College of Chemistry and Materials Science, Anhui Normal University, Wuhu, 241002, China*

[b]*State Key Laboratory of Structural Chemistry, Fujian Institute of Research on the Structure of Matter, Chinese Academy of Sciences, Fuzhou 350002, P. R. China*

[c]*College of Science, Nanjing Agricultural University, Nanjing 210095, P. R. China.*

[d]*School of Chemistry and Chemical Engineering, Yangzhou University, Yangzhou, Jiangsu 225002, P. R. China*

[e]*College of Chemistry and Environmental Science, Hebei University, Baoding 071002, China.*

Corresponding Author

E-mail: yandong8@ahnu.edu.cn

Supporting Information

Section S1 Materials and Methods.

Reagents and Instruments

The raw materials of $Na_2B_4O_7·5H_2O$ (Macklin Chemistry Co., Ltd., 99.5%), $C_4H_2O_4$ (Macklin Chemistry Co., Ltd., 98%) and CF_3COOH (Macklin Chemistry Co., Ltd., 99.0%) were used without further purification.

Colorless single crystals of $Na_2(C_4O_4)(H_3BO_3)(H_2O)_4·H_3BO_3$ were synthesized using a mild hydrothermal method. The added reagents were $Na_2B_4O_7·5H_2O$ (0.2916 g, 1 mmol), $C_4H_2O_4$ (0.1145 g, 1 mmol), CF_3COOH (0.2 mL), and deionized water (4 mL), respectively. The raw reagents were mixed in a 23 mL Teflon-lined autoclave, and then the autoclave was heated to 220 degrees Celsius in three hours and maintained for two days, then cooled to room temperature at a rate of 10 degrees Celsius per hour. Block crystals of **1** were disposed via filtration, which were washed with deionized water, and dried in air (65% yield based on Na). *Anal. Calcd* for **1** (M_r = 353.75): C, 13.58%; H, 3.99%; O, 63.32%; B, 6.11%; Na, 13.00%. Found: C, 13.39%; H, 3.83%; O, 63.75%; B, 5.93%; Na, 12.89%. The crystallographic data, important bond lengths and bond angles are presented in Table **S1–4**. As shown in **Figure S1**, the experimental powder X–ray diffraction data (XRD) pattern was consistent with that simulated from the single crystal XRD data.

Powder X-ray diffraction (PXRD) patterns were collected in the 2θ range of 5°−60° with a step size of 0.02° on a Panalytical X'pert Pro MPD diffractometer equipped with graphitemonochromated Cu Kα radiation. A field emission scanning electron microscope (JSM6700F) equipped with an energy-dispersive X-ray spectroscope (Oxford INCA) was used for microprobe elemental analyses. In the range of 4000−400 cm^{-1}, IR spectra were recorded on a Magna 750 FT-IR spectrometer as KBr pellets. At room temperature, a PerkinElmer Lambda 950 UV−vis−NIR spectrophotometer was used to measure the UV−vis−NIR optical diffuse reflectance spectra. A $BaSO_4$ plate was used as a standard (100% reflectance). The Kubelka−Munk function $F(R) = (1-R)^2/2R = \alpha/S$ was used for the calculation of the absorption (α/S) data from the reflectance spectra, where α is the absorption coefficient, R is the reflectance, and S is the scattering coefficient which is practically wavelength independent when the particle size is larger than 5 μm.[1-2] According to the intercept by extrapolating the

straightest line to the *hv* axis in the *α*/*S* versus *hv* plot, the band gaps were calculated. Under nitrogen atmosphere, a NETZSCH STA449C instrument was used to simultaneously measure thermogravimetric analysis (TGA) at a heating rate of 5 °C min^{-1}. Using an Ultima 2 simultaneous inductively coupled plasma (ICP) optical emission spectrometer, the ICP elemental analysis on K was performed. A German Elementary Vario EL III instrument was used to perform the elemental analyses on C, H, and O elements.

Crystal Structure Determinations

$Na_2(C_4O_4)(H_3BO_3)(H_2O)_4 \cdot H_3BO_3$ was collected by using a SuperNova Dual Wavelength CCD diffractometer with a monochromatic Mo Kα radiation (λ = 0.71073 Å) at 273 K. All datasets and absorption were corrected by the Lorentz and polarization factors and a multi-scan method. On the basis of full matrix least-squares fitting on F^2 using SHELX-97, the structure was solved by using the direct method and refined.[3] All of the non-hydrogen atoms were refined anisotropically. The hydrogen atoms bonded to carbon atoms were refined with isotropic thermal parameters and located at geometrically calculated positions. The H-atoms associated with water molecules in $Na_2(C_4O_4)(H_3BO_3)(H_2O)_4 \cdot H_3BO_3$ were included in the final refinements. The Flack factor is refined to be 0.51 (2) for $Na_2(C_4O_4)(H_3BO_3)(H_2O)_4 \cdot H_3BO_3$, indicating that there exists a small degree of racemic twinning in $Na_2(C_4O_4)(H_3BO_3)(H_2O)_4 \cdot H_3BO_3$.[4-5] For checking the correctness of the space group adopted by these compounds, the program PLATON was applied.[6]

Second harmonic generation measurements

Powder SHG measurements of $Na_2(C_4O_4)(H_3BO_3)(H_2O)_4 \cdot H_3BO_3$ were performed with a Q-switched Nd:YAG laser of 1064 nm by using the method of Kurtz and Perry at room temperature.[7] The SHG effect depends intensely on the particle size, and $Na_2(C_4O_4)(H_3BO_3)(H_2O)_4 \cdot H_3BO_3$ crystalline samples were sieved into the following particle sizes: 45–75, 75–105, 105–150, 150–200, and 200–250 μm. Sieved KDP samples in the same particle-size ranges were used as references. Since $Na_2(C_4O_4)(H_3BO_3)(H_2O)_4 \cdot H_3BO_3$ belongs to *mm*2 point group and three nonvanishing independent tensors left ($d_{113} = d_{311}$, $d_{223} = d_{322}$, d_{333}),[7] effective SHG tensor d_{eff} can be simplified as:

$$\langle d^2 \rangle = \frac{19}{105} d_{333}^2 + \frac{13}{105} d_{333}(d_{311} + d_{322}) + \frac{44}{105}(d_{113}^2 + d_{223}^2) + \frac{26}{105} d_{113} d_{322}$$

Computational Descriptions

The structure of $Na_2(C_4O_4)(H_3BO_3)(H_2O)_4 \cdot H_3BO_3$ determined from single-crystal XRD analysis were adopted in the theoretical calculations. The band structures, densities of states (DOS), and optical dielectric constants of $Na_2(C_4O_4)(H_3BO_3)(H_2O)_4 \cdot H_3BO_3$ were calculated based on density functional theory (DFT) with CASTEP module implemented in the Materials Studio package.[8-10] The valence electrons were treated as H: $1s^1$, C: $2s^2 2p^2$, O: $2s^2 2p^4$, B: $2s^2 2p^3$ and Na: $2s^2 2p^6$. The plane-wave cutoff energy is 517.0 eV. The numerical integration of the Brillouin zone was performed by utilizing Monkhorst−Pack *k*-point meshes 4×4×2. The Fermi level (E_f = 0 eV) was chosen as the reference. In order to make the calculated electronic structure closer to the actual situation, we set the scissors operator value as 0.5 eV.

The optical properties were calculated and are described in terms of the complex dielectric function $\varepsilon(\omega) = \varepsilon_1(\omega)+i\varepsilon_2(\omega)$. The imaginary part of the dielectric function $\varepsilon_2(\omega)$ is given by Equation (1):[11-12]

$$\varepsilon_2(\omega) = \frac{2e^2\pi}{\Omega\varepsilon_0}\sum_{K,V,C} |< \Psi_K^C |\hat{u}\cdot r|\Psi_K^V > |^2 \delta\left(E_K^C - E_K^V - E\right) \quad (1)$$

where $\delta\left(E_K^C - E_K^V - E\right)$ defines the energy difference between the conduction and valence bands at the *k* point with absorption of energy *E*, $\hat{u}$ denotes the polarization of the incident electric field, Ω is the volume of the primitive cell, *e* is the electric charge, and Ψ_K^C and Ψ_K^V are the vectors defining the conduction and valence band wave functions at *k*, respectively. And $\varepsilon_1(\omega)$ can be obtained by using the dispersion relationship of Kramers–Kronig:

$$\varepsilon_1(\omega) = 1 + \frac{2}{\pi}P\int_0^\infty \frac{\omega'\varepsilon_2(\omega')}{\omega'^2 - \omega^2}d\omega' \quad (2)$$

The *P* in front of the integral means the principal value. The first-order nonresonant susceptibility at the low-frequency region is given by $\chi^{(1)}(\omega) = \varepsilon_1(\omega)-1$, and the second-order susceptibilities can be expressed in terms of the first-order susceptibilities as follows:[13]

$$\chi_{ijk}^{(2)}(\omega_3, \omega_1, \omega_2) = \frac{ma}{N^2e^3}\chi_{ii}^{(1)}(\omega_3)\,\chi_{jj}^{(1)}(\omega_1)\chi_{kk}^{(1)}(\omega_2), \quad (3)$$

Table S1. Summary of crystallographic data and structure refinement parameters for $Na_2(C_4O_4)(H_3BO_3)(H_2O)_4 \cdot H_3BO_3$.

Empirical formula	$B_2C_4H_{14}Na_2O_{14}$
Formula weight	353.75
Crystal system	Orthorhombic
Space group	$Cmc2_1$
a (Å)	6.9595(4)
b (Å)	16.1485(14)
c (Å)	12.5850(11)
α (°)	90
β (°)	90
γ (°)	90
V (Å^3)	1414.37(19)
Z	4
D_{cal}(g cm^{-3})	1.661
μ(mm^{-1})	0.214
θ range (°)	3.187–27.500
GOF on F^2	1.050
$R_1{}^a$ [$I > 2\sigma(I)$]	0.0349
$wR_2{}^b$ [$I > 2\sigma(I)$]	0.0671
$R_1{}^a$ (all data)	0.0609
$wR_2{}^b$ (all data)	0.0753
Flack parameter x	0.51(2)

$^aR_1 = \sum||F_o|-|F_c||/\sum|F_o|$, $wR_2 = \{\sum w[(F_o)^2-(F_c)^2]^2/\sum w[(F_o)^2]^2\}^{1/2}$

Table S2. Selected bond lengths (Å) for $Na_2(C_4O_4)(H_3BO_3)(H_2O)_4 \cdot H_3BO_3$.

Na(1)-O(2)	2.338(3)	B(1)-O(2)	1.365(4)
Na(1)-O(4)	2.3461(17)	B(1)-O(3)	1.356(4)
Na(1)-O(4)#1	2.3461(17)	B(2)-O(10)	1.349(4)
Na(1)-O(5)	2.3452(16)	B(2)-O(11)	1.378(4)
Na(1)-O(5)#1	2.3452(16)	B(2)-O(12)	1.362(4)
Na(1)-O(6)	2.376(2)	C(1)-O(6)	1.241(4)
Na(2)-O(3)	2.499(3)	C(2)-O(7)	1.240(4)
Na(2)-O(4)#2	2.3685(17)	C(3)-O(8)	1.271(4)
Na(2)-O(4)#3	2.3685(17)	C(4)-O(9)	1.262(4)
Na(2)-O(5)	2.3369(17)	C(1)-C(2)	1.482(4)
Na(2)-O(5)#1	2.3369(17)	C(1)-C(3)	1.452(4)
Na(2)-O(7)	2.357(3)	C(2)-C(4)	1.464(4)
B(1)-O(1)	1.360(4)	C(3)-C(4)	1.455(4)

[a]Symmetry transformations used to generate equivalent atoms:
#1 -x+1, y, z; #2 -x+1, -y+1, z+1/2; #3 x, -y+1, z+1/2.

Table S3. Important bond angles (°) for $Na_2(C_4O_4)(H_3BO_3)(H_2O)_4 \cdot H_3BO_3$.

Na(1)-O(4)-Na(2)#2	89.00(6)	O(5)-Na(2)-O(5)#1	95.48(9)
Na(2)-O(5)-Na(1)	84.74(6)	O(5)-Na(2)-O(7)	94.84(7)
O(2)-Na(1)-O(4)	94.28(6)	O(7)-Na(2)-O(3)	174.80(11)
O(2)-Na(1)-O(4)#1	94.28(6)	O(7)-Na(2)-O(4)#3	96.88(7)
O(2)-Na(1)-O(5)	84.88(6)	O(7)-Na(2)-O(4)#4	96.88(7)
O(2)-Na(1)-O(5)#1	84.88(6)	O(6)-C(1)-C(2)	135.7(3)
O(2)-Na(1)-O(6)	167.80(10)	O(6)-C(1)-C(3)	134.6(3)
O(4)#1-Na(1)-O(6)	94.31(6)	O(7)-C(2)-C(1)	136.3(3)
O(4)#3-Na(2)-O(3)	86.80(7)	O(7)-C(2)-C(4)	134.6(3)
O(4)#3-Na(2)-O(4)#4	89.27(8)	O(8)-C(3)-C(1)	133.6(3)
O(4)#4-Na(2)-O(3)	86.80(7)	O(8)-C(3)-C(4)	135.7(3)
O(4)-Na(1)-O(4)#1	90.36(8)	O(9)-C(4)-C(2)	133.4(3)
O(4)-Na(1)-O(6)	94.31(6)	O(9)-C(4)-C(3)	136.3(3)
O(5)#1-Na(1)-O(4)	87.29(5)	O(1)-B(1)-O(2)	118.7(3)
O(5)#1-Na(1)-O(4)#1	177.44(7)	O(3)-B(1)-O(2)	116.1(3)
O(5)#1-Na(1)-O(5)	95.03(8)	O(3)-B(1)-O(1)	125.2(3)
O(5)#1-Na(1)-O(6)	86.90(6)	O(10)-B(2)-O(11)	118.5(3)
O(5)#1-Na(2)-O(3)	81.69(6)	O(10)-B(2)-O(12)	126.0(3)
O(5)#1-Na(2)-O(4)#3	167.91(8)	O(12)-B(2)-O(11)	115.6(3)
O(5)#1-Na(2)-O(4)#4	86.44(5)	C(1)-C(3)-C(4)	90.7(2)
O(5)#1-Na(2)-O(7)	94.84(7)	C(3)-C(1)-C(2)	89.8(2)
O(5)-Na(1)-O(4)	177.44(7)	C(3)-C(4)-C(2)	90.3(2)
O(5)-Na(1)-O(4)#1	87.29(5)	C(4)-C(2)-C(1)	89.2(2)
O(5)-Na(1)-O(6)	86.89(6)	C(1)-O(6)-Na(1)	138.2(2)
O(5)-Na(2)-O(3)	81.69(6)	C(2)-O(7)-Na(2)	127.2(2)
O(5)-Na(2)-O(4)#3	86.44(5)	B(1)-O(2)-Na(1)	132.6(2)
O(5)-Na(2)-O(4)#4	167.92(8)	B(1)-O(3)-Na(2)	131.5(2)

[a]Symmetry transformations used to generate equivalent atoms:
#1 -x+1, y, z; #2 -x+1, -y+1, z-1/2; #3 -x+1, -y+1, z+1/2; #4 x, -y+1, z+1/2.

Table S4. Atomic coordinates ($\times 10^4$) and equivalent isotropic displacement parameters ($A^2 \times 10^3$) for $Na_2(C_4O_4)(H_3BO_3)(H_2O)_4 \cdot H_3BO_3$. U_{eq} is defined as one third of the trace of the orthogonalized U_{ij} tensor.

Atom	*x*	*y*	*z*	U_{eq}
Na(1)	5000	5105(1)	2962(1)	29(1)
Na(2)	5000	4568(1)	5372(1)	30(1)
O(8)	5000	1757(1)	1903(2)	33(1)
O(1)	5000	7534(1)	4914(2)	41(1)
O(12)	0	3986(1)	1504(2)	34(1)
O(9)	5000	1216(1)	4411(2)	33(1)
O(11)	0	3631(1)	3288(2)	33(1)
O(7)	5000	3126(1)	5089(2)	37(1)
O(5)	7485(2)	4835(1)	4171(1)	33(1)
O(4)	2609(2)	5413(1)	1710(1)	34(1)
O(6)	5000	3664(1)	2589(2)	40(1)
O(2)	5000	6431(1)	3706(2)	40(1)
O(10)	0	2552(2)	2045(2)	43(1)
O(3)	5000	6112(2)	5492(2)	40(1)
C(4)	5000	1889(2)	3902(2)	25(1)
C(2)	5000	2760(2)	4223(2)	26(1)
C(3)	5000	2133(2)	2789(2)	25(1)
C(1)	5000	3001(2)	3088(3)	27(1)
B(1)	5000	6705(2)	4731(3)	28(1)
B(2)	0	3372(2)	2246(3)	30(1)

Table S5. The assignments of the infrared absorption peaks for $Na_2(C_4O_4)(H_3BO_3)(H_2O)_4 \cdot H_3BO_3$.

Assignments	Absorption bands (cm^{-1})
asymmetric stretching of H-O	3540-3089
in-plane bending of the B-O-H groups	2381,2261
the bending of group H-O-H	1640,1604
asymmetric stretching of B-O	1527,1481
deformation vibration of C-(C=)-C	1208,1126
symmetric stretching of B-O	879,831
plane bending of the $[BO_3]^{3-}$ triangles	671-547

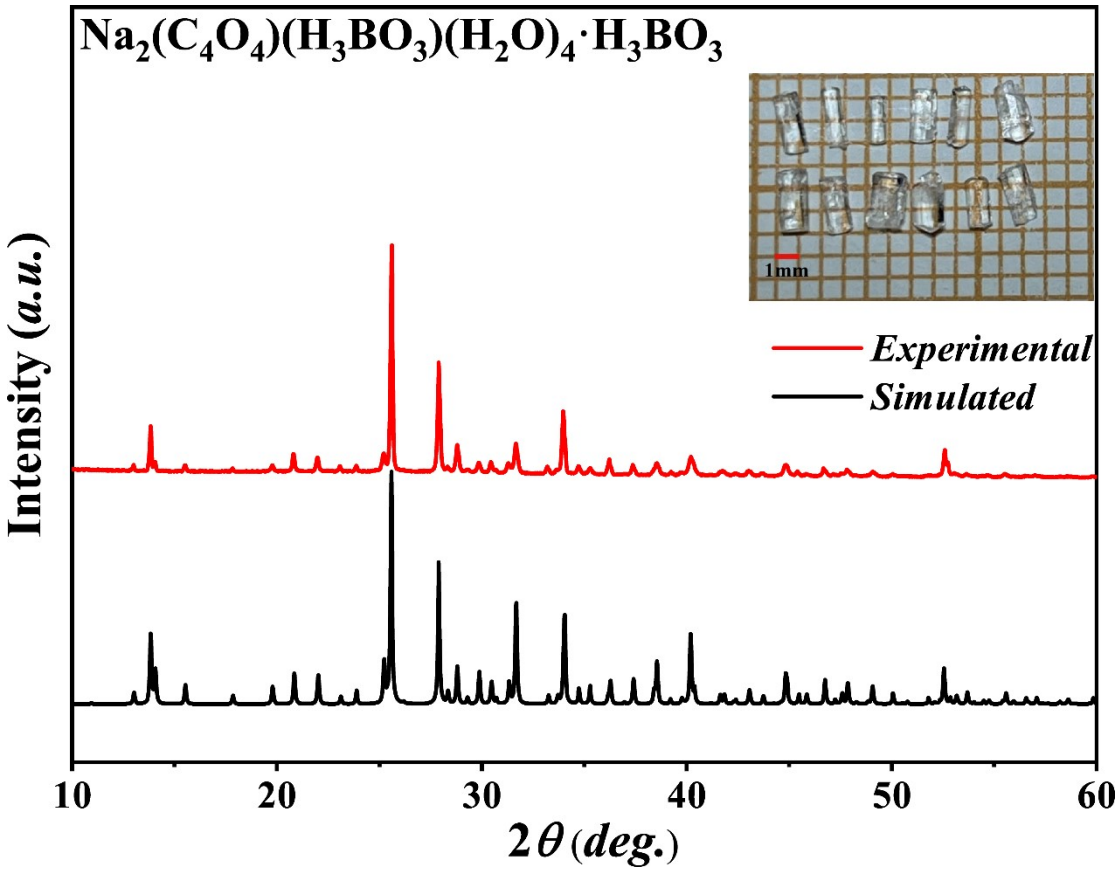

Figure S1. Experimental and calculated XRD patterns for $Na_2(C_4O_4)(H_3BO_3)(H_2O)_4{\cdot}H_3BO_3$, inset shows selected crystals photograph.

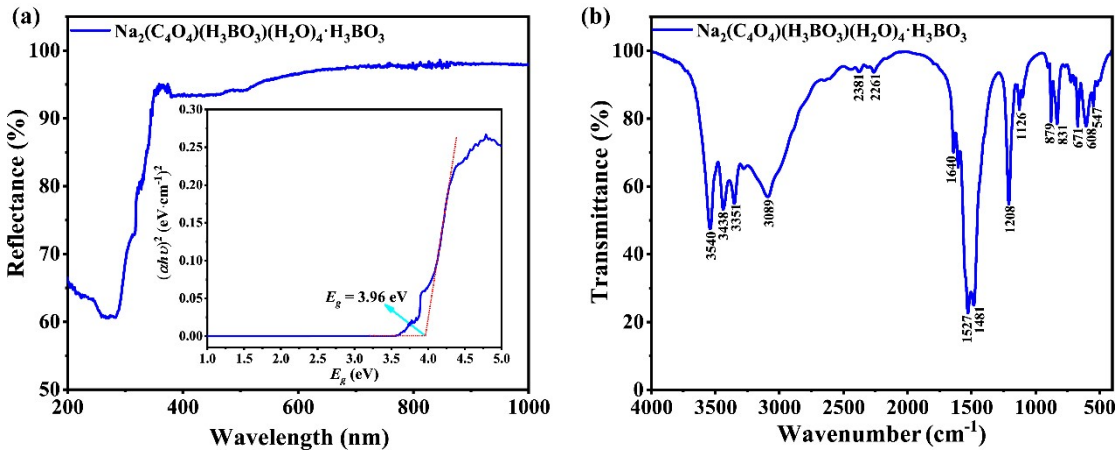

Figure S2. The UV-vis diffuse reflectance spectrum (a) and infrared (IR) spectrum (b) of $Na_2(C_4O_4)(H_3BO_3)(H_2O)_4{\cdot}H_3BO_3$.

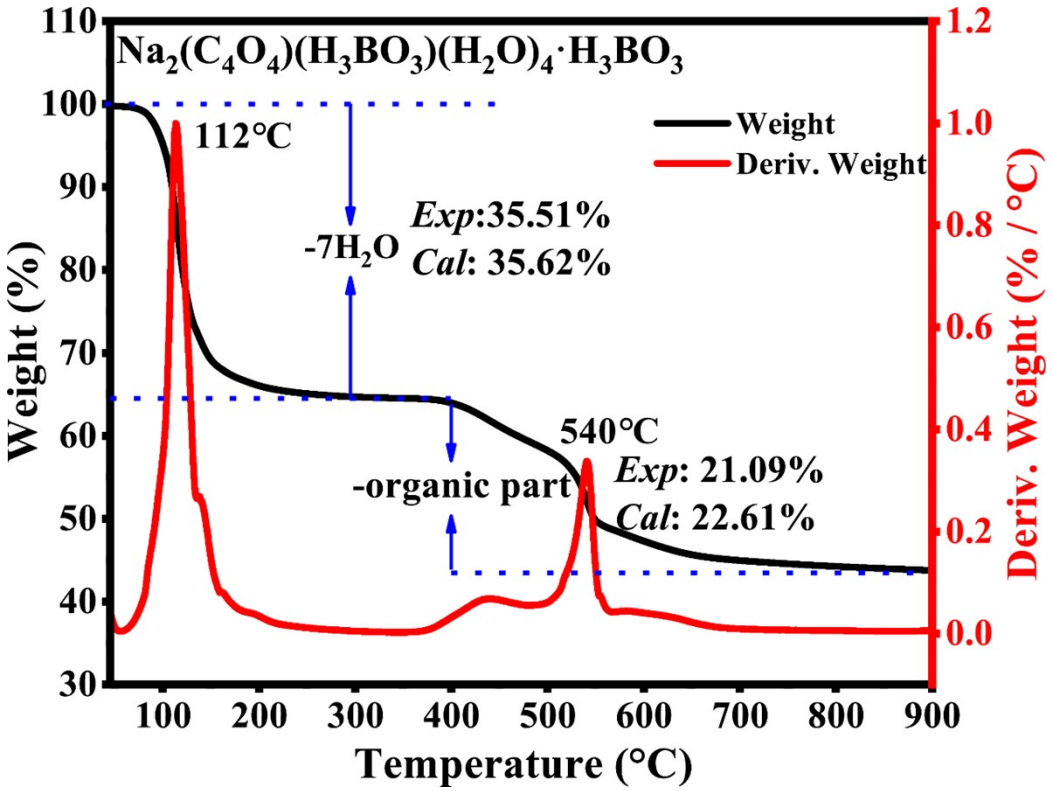

Figure S3. TGA and DTA curves for $Na_2(C_4O_4)(H_3BO_3)(H_2O)_4 \cdot H_3BO_3$.

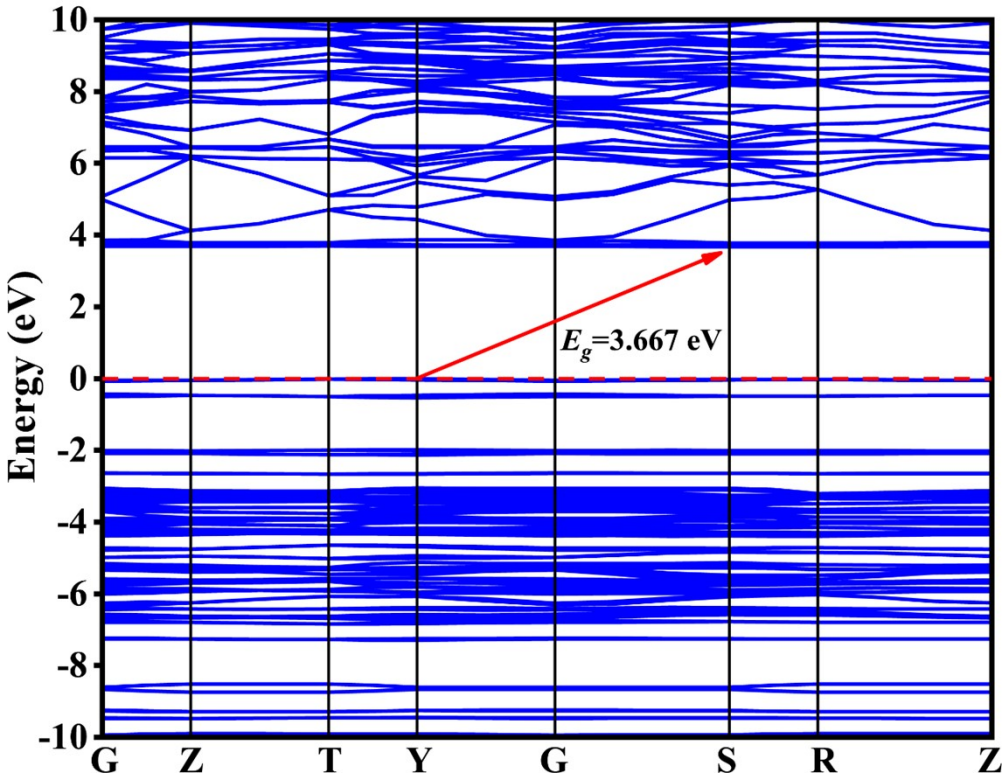

Figure S4. Calculated band structure for $Na_2(C_4O_4)(H_3BO_3)(H_2O)_4 \cdot H_3BO_3$.

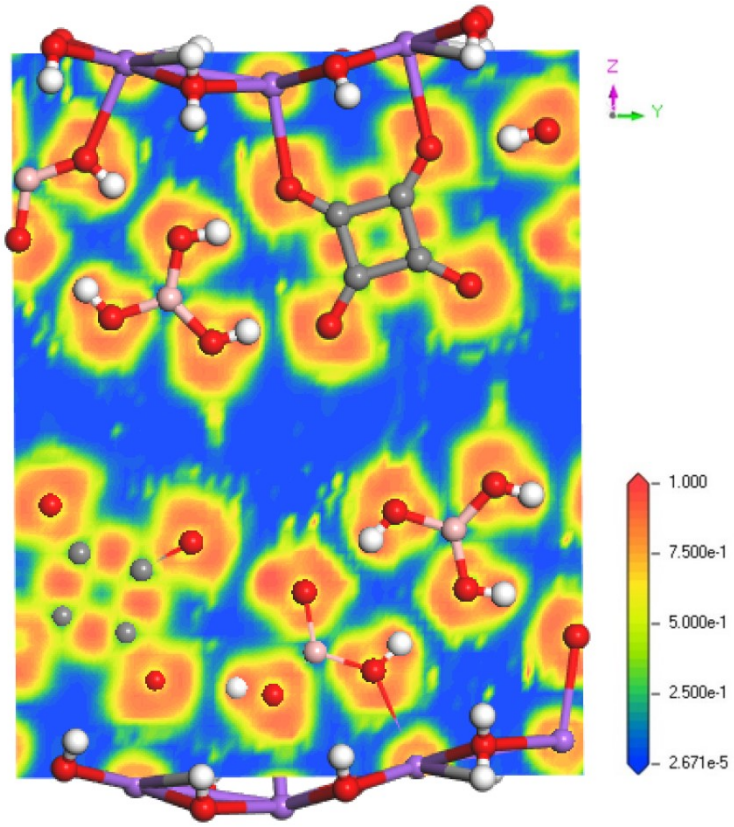

Figure S5. The (100) projection of the electron localization function (ELF) for $Na_2(C_4O_4)(H_3BO_3)(H_2O)_4 \cdot H_3BO_3$.

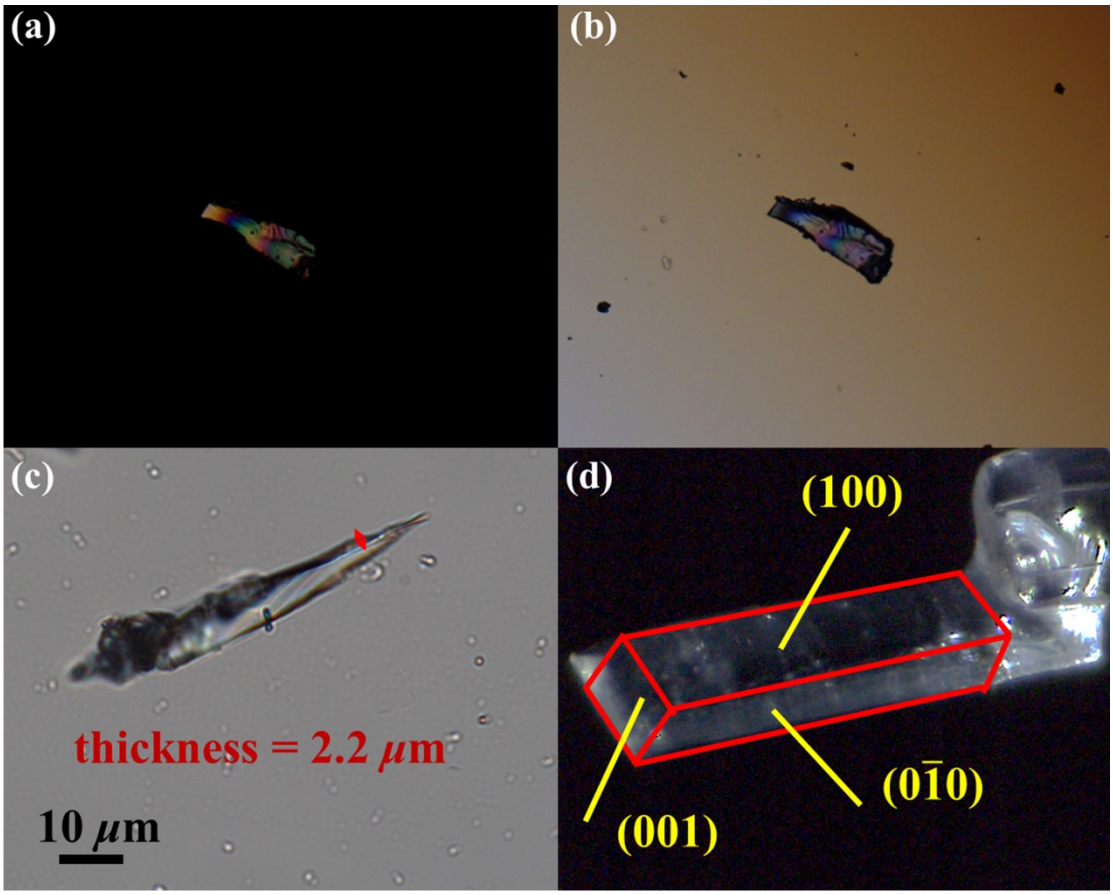

Figure S6. (a) Original interference color of the $Na_2(C_4O_4)(H_3BO_3)(H_2O)_4 \cdot H_3BO_3$ crystal under orthogonal polarized light. (b) $Na_2(C_4O_4)(H_3BO_3)(H_2O)_4 \cdot H_3BO_3$ crystal under complete extinction. (c) Thickness of the selected $Na_2(C_4O_4)(H_3BO_3)(H_2O)_4 \cdot H_3BO_3$ crystal plate. (d) Crystal orientation of the $Na_2(C_4O_4)(H_3BO_3)(H_2O)_4 \cdot H_3BO_3$ crystal indexed by single-crystal XRD measurement.

Reference

1 Tauc, J. Absorption edge and internal electric fields in amorphous semiconductors. *Mater. Res. Bull*. **1970**, *5*, 721.

2 Kubelka, P.; Munk, F. An article on optics of paint layers. Z. *Tech. Phys*., **1931**, *12*, 886.

3 Sheldrick, G. M. Single-crystal structure validation with the program PLATON SHELXTL Crystallographic Software Package, SHELXTL, version 5.1; Bruker-AXS: Madison, WI, 1998

4 Huang, C.; Hu, C. L.; Xu, X.; Yang, B. P.; Mao, J. G. Explorations of a Series of Second Order Nonlinear Optical Materials Based on Monovalent Metal Gold(III) Iodates. *Inorg. Chem.* **2013**, *52*, 11551−11562.

5 Yu, J.; Liu, L.; Jin, S.; Zhou, H.; He, X.; Zhang, C.; Zhou, W.; Chen, X.; Wang, X.; Chen, C. T. Superstructure and stacking faults in hydrothermal-grown $KBe_2BO_3F_2$ crystals. *J. Solid State Chem.* **2011**, *184*, 2790−2793.

6 Spek, A. L. Single-crystal Structure Validation with the Program PLATON. *J. Appl. Crystallogr*. **2003**, *36*, 7.

7 S. K. Kurtz and T. T. Perry, A Powder Technique for the Evaluation of Nonlinear Optical Materials, *J. Appl. Phys.*,**1968**, *39*, 3798–3813.

8 Segall, M. D.; Lindan, P. J. D.; Probert, M. J.; Pickard, C. J.; Hasnip, P. J.; Clark, S. J.; Payne, M. C. First-principles Simulation: Ideas, Illustrations and the CASTEP code. *J. Phys.: Condens. Matter*. **2000**, *14*, 2717.

9 Payne, M. C.; Teter, M. P.; Allan, D. C.; Arias, T. A.; Joannopoulos, J. D. Iterative Minimization Techniques Forab Initiottotal-energy Calculations: Molecular Dynamics and Conjugate Gradients. *Rev. Mod. Phys.* **1992**, *64*, 1045–1097.

10 Clark, S. J.; Segall, M. D.; Pickard, C. J.; Hasnip, P. J.; Probert, M. I.; Refson, K.; Payne, M. C. First principles methods using CASTEP. *Z. Kristallogr.* **2005**, *220*, 567–570.

11 Bassani, F.; Parravicini, G. P. Electronic States and Optical Transitions in Solids. *Pergamon Press Ltd. Oxford*. **1976**.

12 Gajdoš, M.; Hummer, K.; Kresse, G.; Furthmüller, J.; Bechstedt, F. Linear Optical Properties in the Projector-augmented Wave Methodology. *Phys. Rev. B* **2006**, *73*, 045112.

13 Boyd, R. W. *Nonlinear Optics*; Academic Press: 2003.